Materials Research Proceedings 33 (2023) 177-184 https://doi.org/10.21741/9781644902677-26

Mechanical properties of additively manufactured lattice structures through numerical BCC cell characterisation

Giuseppe Mantegna[1,a *]

[1]Università degli Studi di Enna Kore, Facoltà di Ingegneria e Architettura, Cittadella universitaria, 94100 Enna – Italy

[a]giuseppe.mantegna@unikorestudent.it

Keywords: Additive Manufacturing, Periodicity, 3D Lattice, FEM

Abstract. Additive Manufacturing (AM) technologies have acquired significant attention in the modern industry due to their versatility in creating custom-designed components with complex shapes utilising multiple materials with minimal material waste. Moreover, the full potential of AM technologies relies on creating meta-materials, structured materials with distinctive mechanical properties designed for specific purposes and optimised throughout various regions of the structure. For instance, it is possible to design topology-optimised structures through periodic lattice cells by varying the cell types, dimensions or relative volume fractions [1]. In this way, structures with graded or separate regions can be manufactured in one single manufacturing process, significantly reducing the design-to-production time and allowing a rapid iteration and design optimisation [2]. As previously mentioned, lattice structures are formed by a unit cell properly repeated with an ordered topology to achieve desired mechanical properties. Amongst the different cell types, thanks to its simple configuration and ease of print with AM technologies, the Body-Centered Cubic (BCC) structure is frequently used [3]. Several studies are present in the literature to predict and evaluate the behaviour of this cell type analytically, numerically and by experiments showing its excellent specific mechanical properties [4]–[6]. This paper investigates the mechanical properties of additively manufactured structures, comparing experimental results with numerical simulations conducted using various modelling approaches, including a full 3D model, a simplified 1D and 2D approach, and homogenized models. At first, the mechanical properties of a lattice BCC structure are considered, followed by the investigation of a sandwich structure featuring a lattice core. At this stage, the skins and the core are 3D printed in Polylactic acid PLA; the lattice core structure is composed of BCC unit cells. Finally, the mechanical performances of the AM structures are compared to assess the accuracy and reliability of the different modelling approaches.

Finite Element Analyses

To determine the mechanical properties of the BCC cells and lattice structures, numerical simulations were carried out in the commercial software Ansys. In this study, various modelling approaches are presented to assess the robustness of the models and minimize computational expenses for future simulations on macro-scale structures. More specifically, the study compares full 3D analyses with simplified 1D and 2D models, as well as homogenized models based on the previous analyses' outcomes. Three major numerical configurations are considered. At first the mechanical properties of the single BCC unit cell are evaluated. As a periodic element repeated in the structure, proper periodic and boundary conditions must be ensured for the single BCC cell analyses. For this reason, a specific routine has been developed in Ansys Parametric Design Language (APDL) to ensure a double periodicity on the 3D FEM simulations, while ad-hoc boundary conditions were imposed for the simplified beam 1D models. Subsequently compression tests on a cubic BCC structure are considered followed by bending tests on a sandwich structure consisting of a BCC lattice core sandwiched between two skins.

Materials Research Proceedings 33 (2023) 177-184 https://doi.org/10.21741/9781644902677-26

Single BCC Cell – Compression and Shear tests

Figure 1 displays the single Body-Centered Cubic (BCC) unit cell which serves as the fundamental periodic element for the cubic and sandwich structures. The geometric properties of this BCC unit cell are listed in Table 1. As in other studies [4], [5], due to the bending-dominated behaviour of the BCC cell in compression, the 1D beam model struts are divided into multiple sections to take into account the rigidity of the nodes. According to [4], for a BCC cell, it is possible to retrieve the stiff beam length h_{comp} as a function of the diameter-cell size ratio. However, when the cell is subjected to a shear loading, each strut is both bending and stretched loaded. In this condition, the overmentioned approach has been corrected by numerically calibrating the h-d ratio. For this study, a stiff beam length $h_{shear} = 0.35$ is selected. Further studies are currently being conducted to optimise the length according to the local stress distribution.

Table 1 – BCC Cell nominal size.

Cell size, L [mm]	10.0
Strut diameter, d $[mm]$	2.0
Stiff beam length, h_{comp} $[mm]$[4]	0.93
Stiff beam length, h_{shear} $[mm]$	0.35

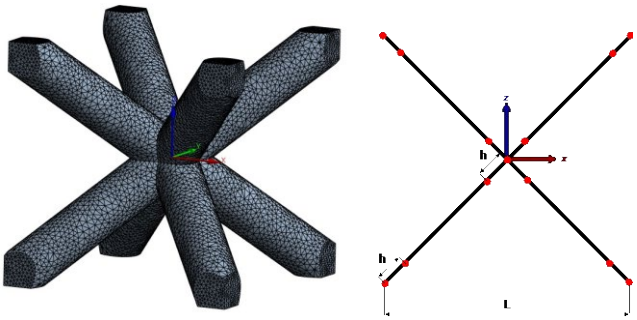

Figure 1 – 3D and 1D BCC cells.

As mentioned, FDM PLA are considered for the numerical analyses whose properties, retrieved on experimental tests performed on dog-bone specimens, are $E = 3132\ MPa$, $\sigma_{yield} = 20\ MPa$ with a density $\rho = 1275\ kg/m^3$.

The 3D models use double periodic conditions along the *x* and *y* directions modelled through constraints equations and implemented through a specific APDL code, as outlined in previous work [7] and schematically shown in Figure 2.a.

Since the 1D model does not have multiple nodes on the lateral faces, periodic conditions are enforced through remote points coupling for the compression test as shown in Figure 3. The boundary conditions used for the compression and shear analyses in both 3D and 1D models are presented in Figure 2.b and Figure 3, respectively.

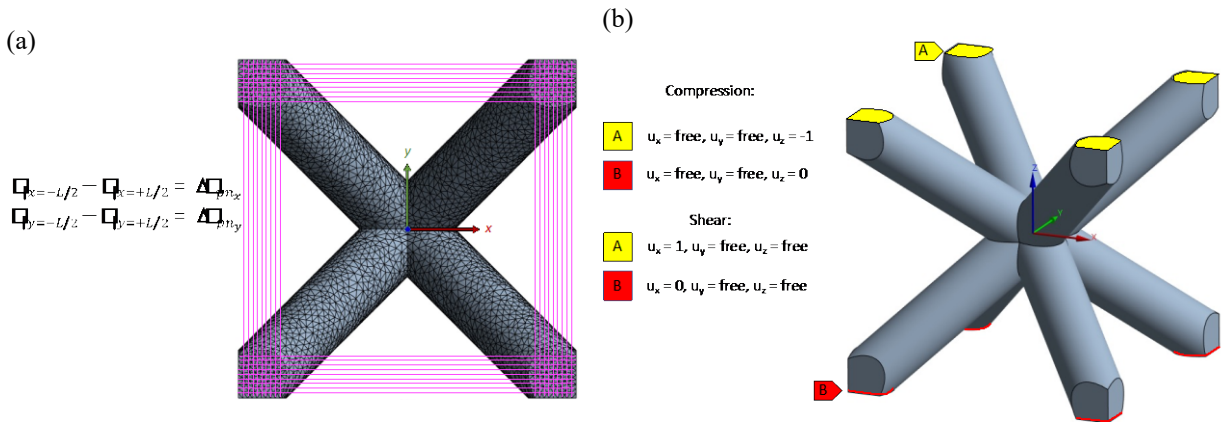

Figure 2 – 3D model Compression/Shear (a) Periodic conditions; (b) Boundary conditions.

Materials Research Proceedings 33 (2023) 177-184 https://doi.org/10.21741/9781644902677-26

Compression	Shear
$h_{comp} = 0.93$ mm	$h_{shear} = 0.35$ mm
$Nodes_{\|z=-L/2}$: u_x = free, u_y = free, u_z = 0	$Nodes_{\|z=-L/2}$: $u_x = 0$, $u_y = 0$, $u_z = 0$
$Nodes_{\|z=+L/2}$: u_x = free, u_y = free, u_z = -1	$Nodes_{\|z=+L/2}$: $u_x = 1$, $u_y = 0$, $u_z = 0$
Fixed Rotation on nodes	
$Nodes_{\|x=-L/2}$: u_x Coupled with RP1	
$Nodes_{\|x=+L/2}$: u_x Coupled with RP2	
$Nodes_{\|y=-L/2}$: u_y Coupled with RP1	
$Nodes_{\|y=+L/2}$: u_x Coupled with RP2	

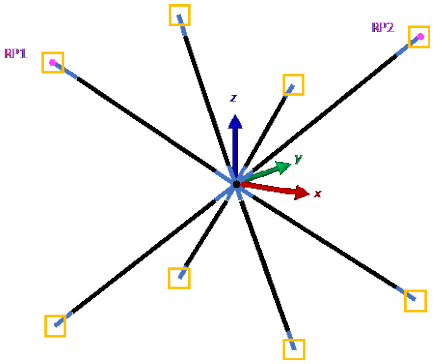

Figure 3 – 1D Compression/Shear Boundary and Periodic conditions

From the 3D, model an equivalent elastic modulus $E^*_{3D} = 23.5\,MPa$ is retrieved with a Poisson's ratio $\nu^*_{3D} = 0.47$ and a shear modulus $G^*_{3D} = 82.4\,MPa$. The simplified 1D model gives an equivalent elastic modulus $E^*_{1D} = 22.6\,MPa$, a Poisson's ratio $\nu^*_{1D} = 0.46$ and a shear modulus $G^*_{1D} = 82.7\,MPa$. The 1D numerical model accurately replicate the behaviour of the 3D numerical, resulting in a significant reduction in computational costs. This reduction is due to the decreased number of model elements, namely 192 elements as opposed to 47192 elements employed in the 3D model. Moreover, the absence of constraints equations that pair each node on the lateral faces of the 3D model contributes significantly to the reduction of computational effort. Figure 4 shows the directional deformation contour maps for the 3D and 1D compression and shear tests.

(a)

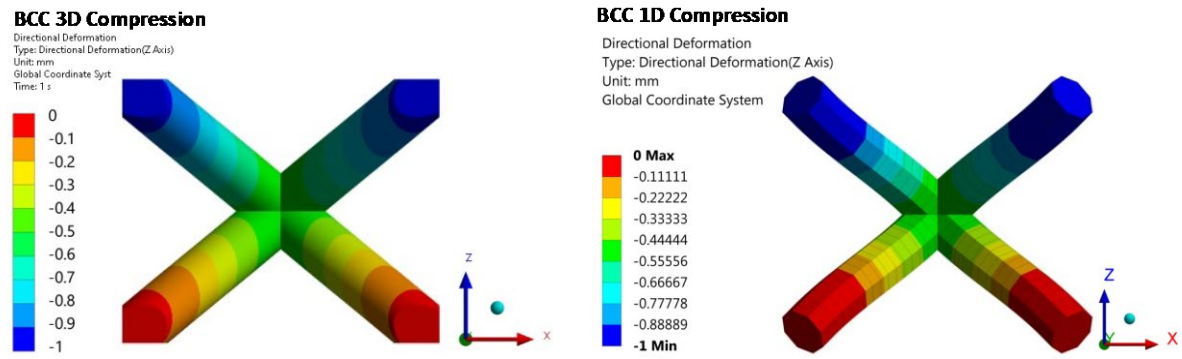

(b)

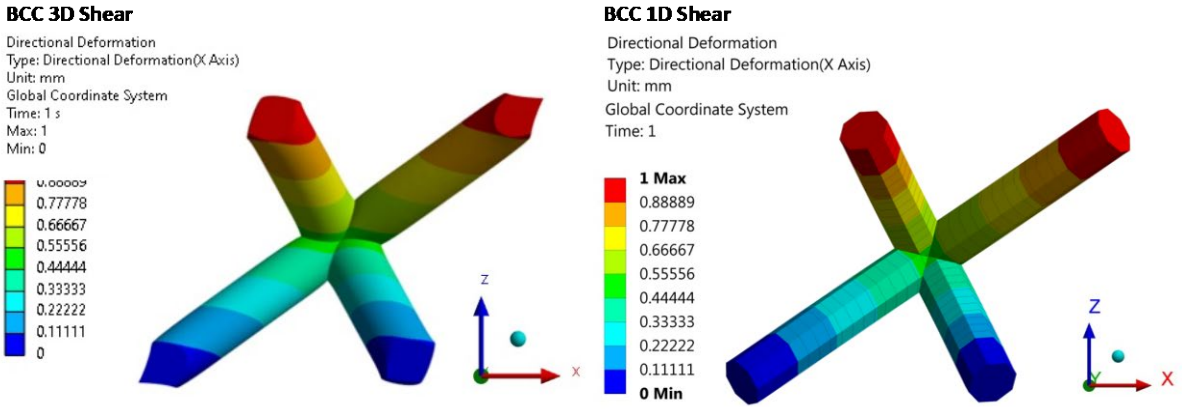

Figure 4 – Directional deformation contour maps of 3D and 1D Compression (a) and Shear (b).

Materials Research Proceedings 33 (2023) 177-184 https://doi.org/10.21741/9781644902677-26

BCC Structure Compression tests

Following the numerical analyses on the single BCC cell, the BCC structure showed in Figure 5 was considered and investigated under a compression loading.

Table 2 – BCC Cell and Coupon nominal size.

Cell size, l [mm]	10.0
Strutt diameter, d $[mm]$	2.0
Stiff beam length, h_{comp} $[mm]$	0.93
Coupon dimensions, $L \times W \times H$ $[mm]$	40x40x40
Coupon Volume fraction, V^*/V	0.1784

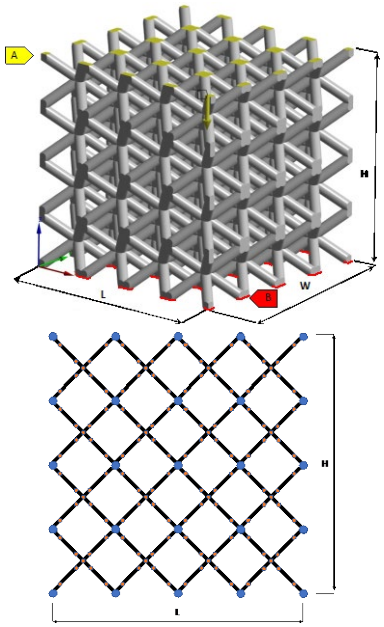

Figure 5 – 3D and 1D Compression coupons.

For this analysis, no periodicity conditions were given. A displacement along the z-direction is given at the top surface (Figure 5, Surface A) while the bottom surface (Figure 5, Surface B) has constrained displacements along the z-direction. Both the 3D and 1D numerical analyses give consistent results with the single BCC cell results: an apparent modulus $E_{3D} = 23.6\,MPa$ and $E_{1D} = 22.7\,MPa$ is retrieved, with a negligible error of 0.4% in relation to the corresponding modulus values obtained from the single BCC cell analyses.

The periodicity and boundary conditions imposed on the 3D and 1D models for the compression test analysis thus give coherent results and can be used to characterise the macro-behaviour of the structure from the unit cell.

The equivalent stress contour map for the 3D model is presented in Figure 6.a while the combined stress for the 1D model is shown in Figure 6.b showing the most stressed areas of the structure despite being different mechanical entities. Similar to the single cell configuration, the compression loading configuration stresses the structure mainly in bending. As expected, the node joints situated at the faces of the coupon are the main locations of stress concentration on both the 1D e 3D model since they are not constrained by other adjacent unit cells outwards of the coupon faces. Notably, in the 3D model, the inner joint area experiences a more elevated stress level in comparison to the outer area, with an increase in stress ranging between 15% to 30%. However, this stress distribution pattern cannot be accurately predicted by the 1D model, which only accounts for a single node located at the strut end and, therefore, does not differentiate between an inner and outer joining area.

Materials Research Proceedings 33 (2023) 177-184 https://doi.org/10.21741/9781644902677-26

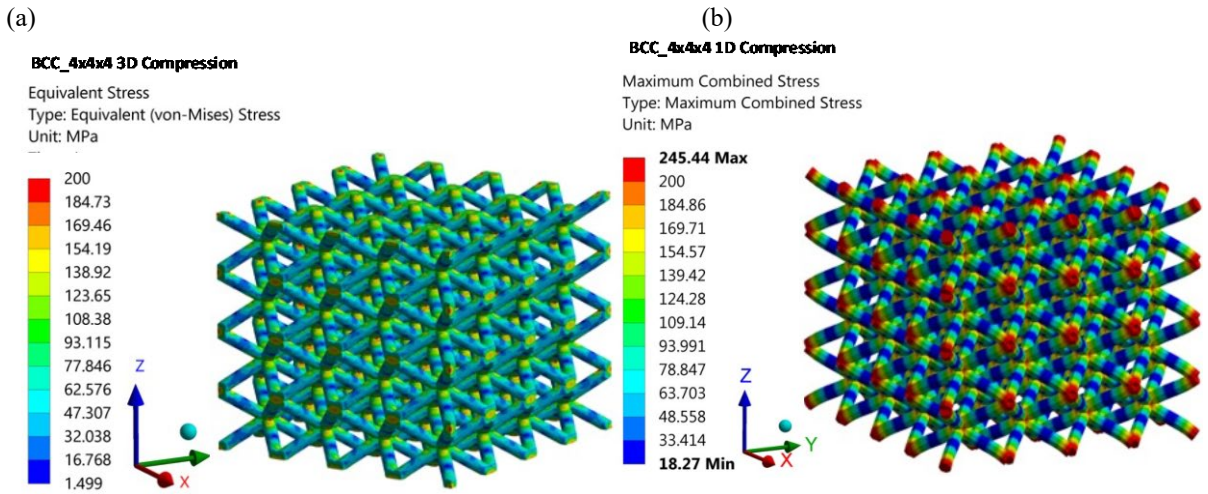

Figure 6 – (a) Equivalent stress 3D model and (b) Maximum combined Stress 1D model contour maps.

Sandwich structure flexure test

A Three Point Bending Test (3PBT) on a sandwich structure is considered as final numerical analysis. More specifically, the sandwich consists of two skins with a nominal thickness of $t_s = 1\,mm$ enclosing a BCC lattice core formed by $20 \times 3 \times 1$ cells with dimension as reported in Table 1.

Three numerical models are considered to study this test, namely 3D model, 1D/2D model and Homogenised model. The homogenised 3D model, Figure 7.a, is composed of three solid plates. The FDM PLA properties previously used are imposed to the two external skins, while the homogenized core is characterized by equivalent mechanical properties obtained from the single cell 3D analysis, namely $E^* = 23.5\,MPa$, $\nu^* = 0.47$ and $G^* = 82.4\,MPa$. As illustrated in Figure 7.b, only half specimen is considered for all of them. A symmetry plane, by constraining the displacements along the *x*-direction is thus imposed.

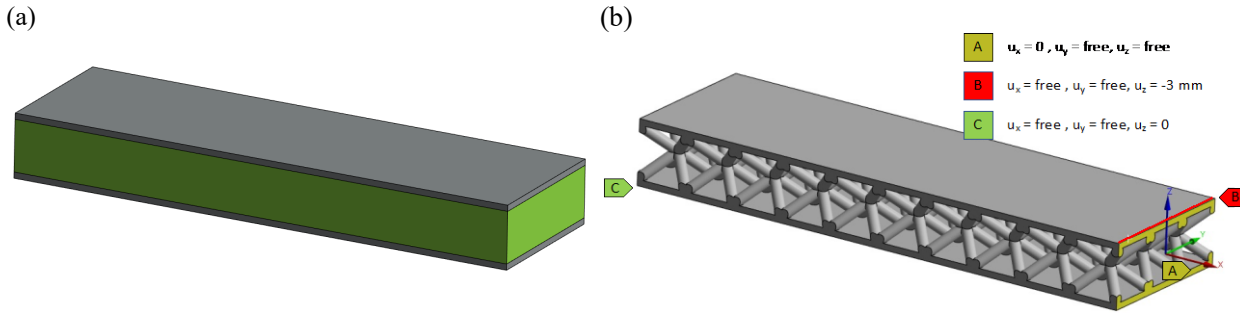

Figure 7 –3PBT Boundary Conditions. (a) 3D homogenised model, (b) 3D model and boundary conditions.

The load-displacement diagram in Figure 8 compares the mechanical response of the three models. The numerical bending rigidities, calculated as $D = Load/Deflection$, for each model are: $D_{3D} = 38.66\,N/mm$, $D_{hom} = 37.97\,N/mm$ and $D_{1D/2D} = 37.36\,N/mm$.

Materials Research Proceedings 33 (2023) 177-184 https://doi.org/10.21741/9781644902677-26

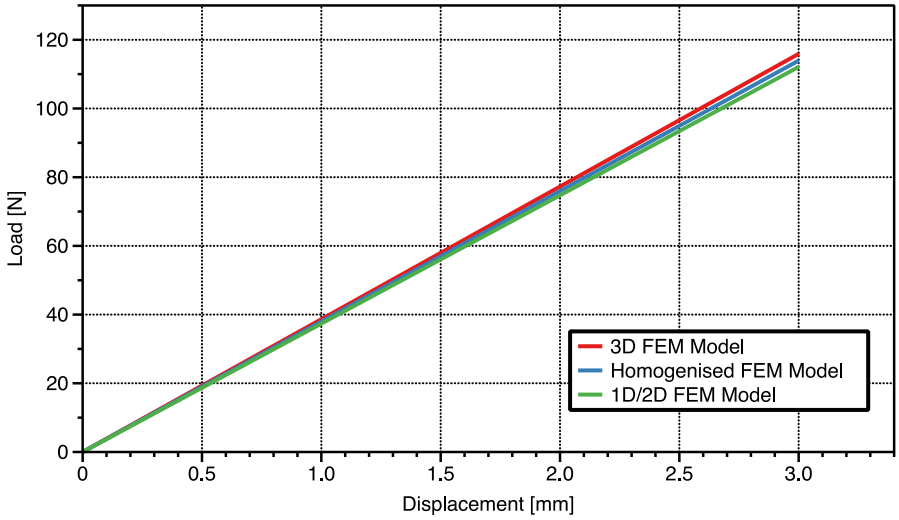

Figure 8 – 3PBT load-displacement diagram, numerical results.

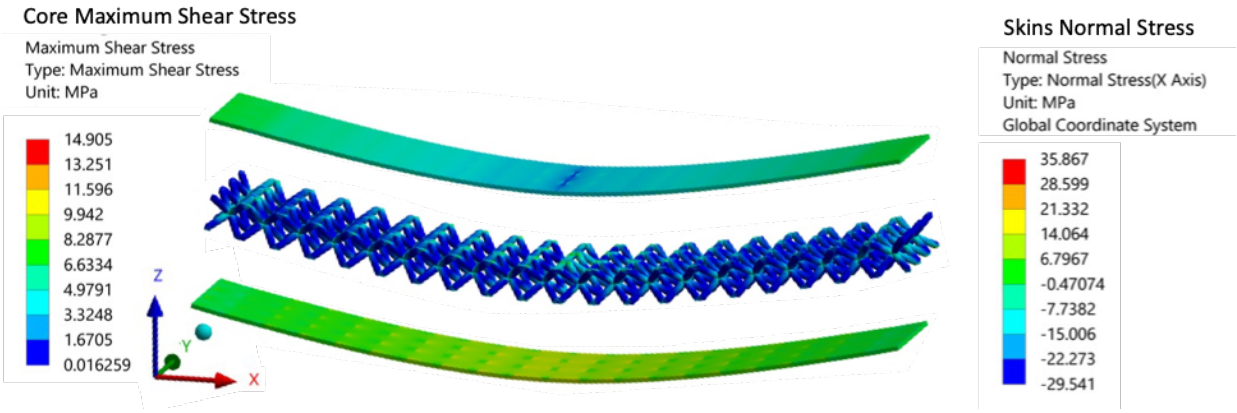

Figure 9 – 3D Stress distribution contour map exploded-view: Core shear stress and Skins normal stress.

The exploded-view in Figure 9 depicts the stress distribution of the sandwich structure, wherein the lower skin experiences compression longitudinal stress, while the upper skin is subjected to compression. Notably, the core bears the highest shear stresses underneath the supports located at the end of the specimen.

Experimental Tests and comparison with numerical results

Compression tests

A series of experimental tests on the 3D coupons was performed to validate the numerical results. The aforementioned coupons were manufactured in Polylactic acid PLA through fused deposition modelling (FDM) with a base print speed of $50\ mm/s$ and a temperature of the extruder of $200\ °C$. For the sake of reproducibility, three coupons were tested.

The compression response of the BCC coupons was compared with the numerical results in Figure 10. The graph depicts three distinct phases of lattice structures under compression, which are consistent with previous research findings [5], [8]. The linear elastic regime is visible in the initial section of the graph, followed by an elastic-plastic collapse at the centre. The right-hand side of the diagram, characterized by a steep increase in stress, corresponds to the densification phase. Table 3 summarise the mechanical properties retrieved from the experimental tests. A high level of correspondence between the numerical and experimental results is evident, with a 4.5% error for the 3D model and a negligible 0.5% error for the 1D model.

Materials Research Proceedings 33 (2023) 177-184 https://doi.org/10.21741/9781644902677-26

Table 3 – Experimental compression tests results.

Weight [g]	Relative density	Equivalent Young Modulus [MPa]	Equivalent Yield Modulus [MPa]	Maximum Strength [MPa]
14.617	0.1791	21.06	0.76	1.01
14.67	0.1797	23.56	0.83	1.17
14.65	0.1795	23.11	0.80	1.20

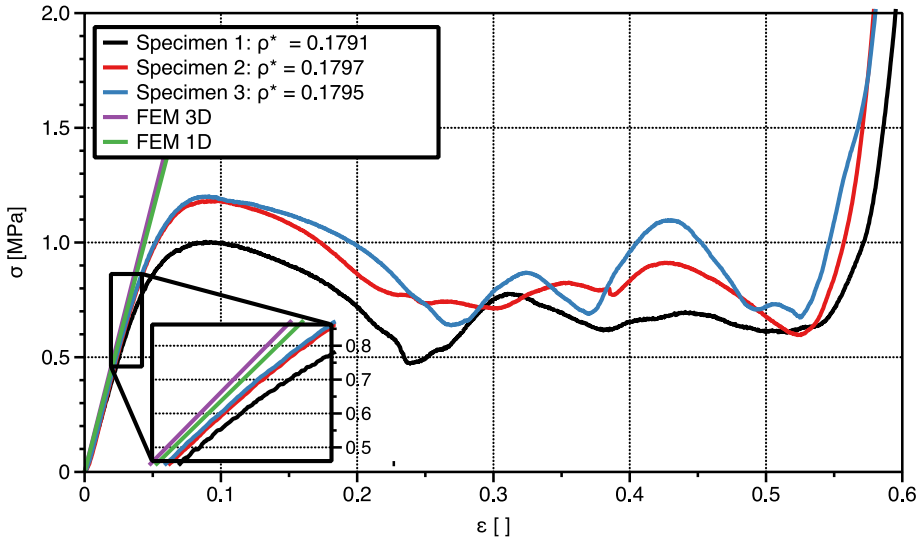

Figure 10 - Compression tests: Numerical-experimental stress-strain curves comparison.

During the experimental tests, the first and second specimens showed a shear deformation band, as depicted in Figure 11.a and Figure 11.b, as a result of compressive buckling that provoked the diagonal shear deformation. The third sample, on the other hand, showed a uniform layer-by-layer failure from the uppermost layers and subsequently propagating to the lower layers, with the central region remaining intact until the final stages of the deformation process.

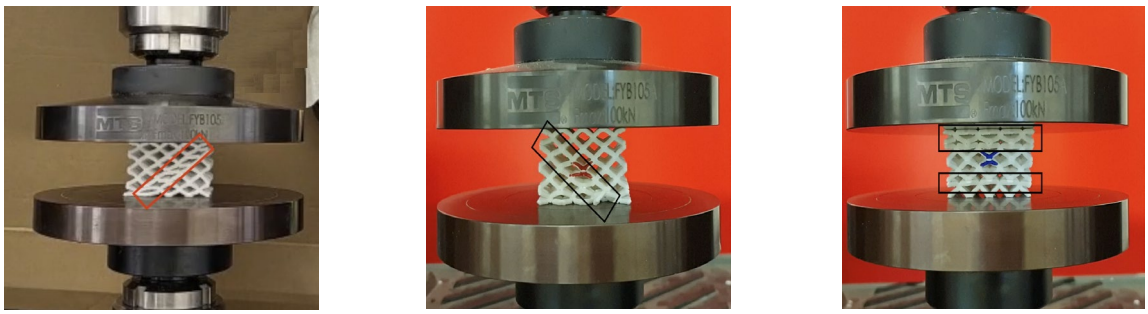

Figure 11 – Deformation modes of BCC lattice structure. Shear bands details.

Three-Point bending test

An experimental test of the 3PBT was also performed to check the validity of the numerical results. The test arrangement, shown in Figure 12.b , considers a span between the supports is $S = 200\ mm$ while the load is applied in the centre of the specimen.

Figure 12.a compares the experimental load-displacement curve with the numerical simulation results revealing an experimental bending rigidity of the sandwich of $D = 34\ N/mm$. A relative error of 13%, 11% and 9% is thus recorded between the 3D, homogenised and 1d/2D FEM model respectively.

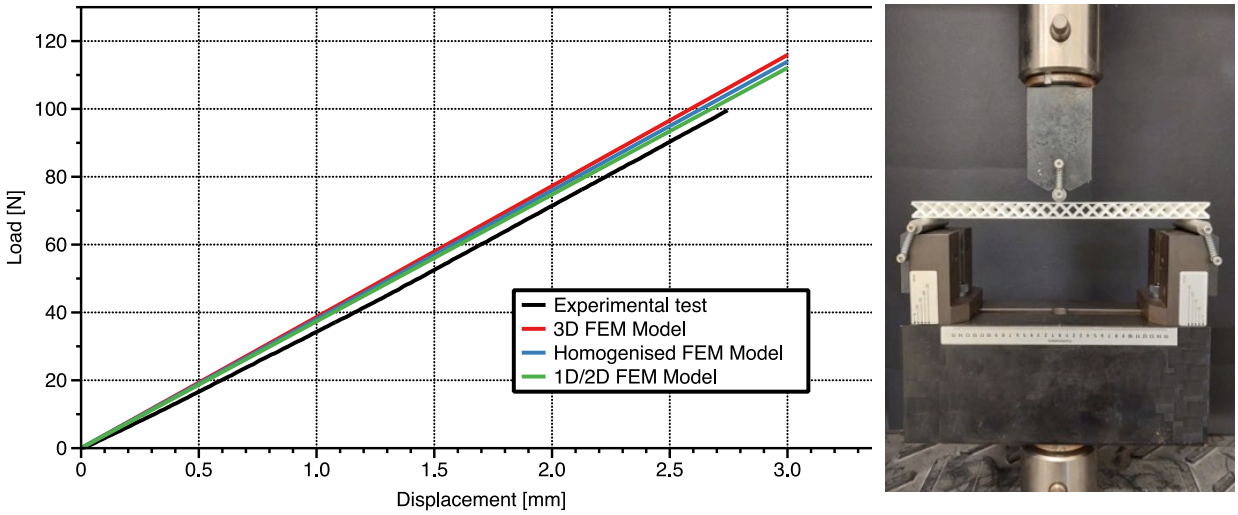

Figure 12 – Experimental bending test. Load-Displacement diagram and experimental test setup.

References

[1] J. J. Sobczak and L. Drenchev, "Metallic Functionally Graded Materials: A Specific Class of Advanced Composites," *J Mater Sci Technol*, vol. 29, no. 4, pp. 297–316, Feb. 2013. https://doi.org/10.1016/j.jmst.2013.02.006

[2] A. Bandyopadhyay and B. Heer, "Additive manufacturing of multi-material structures," *Materials Science and Engineering R: Reports*, vol. 129. Elsevier Ltd, pp. 1–16, Feb. 2018. https://doi.org/10.1016/j.mser.2018.04.001

[3] L. Bai, C. Yi, X. Chen, Y. Sun, and J. Zhang, "Effective design of the graded strut of BCC lattice structure for improving mechanical properties," *Materials*, vol. 12, no. 13, 2019. https://doi.org/10.3390/ma12132192

[4] D. Tumino, A. Alaimo, C. Orlando, S. Valvano, and C. R. Vindigni, "Lattice Core FEM Simulation with a Modified-Beam Approach," *Lecture Notes in Mechanical Engineering*, pp. 946–954, 2023. https://doi.org/10.1007/978-3-031-15928-2_83

[5] R. Gümrük and R. A. W. Mines, "Compressive behaviour of stainless steel micro-lattice structures," *Int J Mech Sci*, vol. 68, 2013. https://doi.org/10.1016/j.ijmecsci.2013.01.006

[6] E. Ptochos and G. Labeas, "Elastic modulus and Poisson's ratio determination of micro-lattice cellular structures by analytical, numerical and homogenisation methods," *Journal of Sandwich Structures and Materials*, vol. 14, no. 5, 2012. https://doi.org/10.1177/1099636212444285

[7] G. Mantegna *et al.*, "Representative volume element homogenisation approach to characterise additively manufactured porous metals, pp. 1–10, Feb. 2022. https://doi.org/10.1080/15376494.2022.2124002

[8] H. Lei *et al.*, "Evaluation of compressive properties of SLM-fabricated multi-layer lattice structures by experimental test and μ-CT-based finite element analysis," *Mater Des*, vol. 169, 2019. https://doi.org/10.1016/j.matdes.2019.107685